1-1-1998

Stray Light Design and Analysis of the Sounding of the Atmosphere Using Broadband Emission Radiometry (SABER) Telescope

John L. Stauder

Roy W. Esplin

Stauder, John L., and Roy W. Esplin. 1998. "Stray Light Design and Analysis of the Sounding of the Atmosphere Using Broadband Emission Radiometry (SABER) Telescope." *Proceedings of SPIE* 3437: 52–59. doi:10.1117/12.331334.

Stray light design and analysis of the Sounding of the Atmosphere using Broadband Emission Radiometry (SABER) telescope

John L. Stauder and Roy W. Esplin

Space Dynamics Laboratory, Utah State University, Logan, UT 84321

ABSTRACT

The Sounding of the Atmosphere using Broadband Emission Radiometry (SABER) instrument is a 10-channel earth limb-viewing sensor that is to measure atmospheric emissions in the spectral range of 1.27 μm to 16.9 μm. Presented in this paper is the stray light design and analysis of SABER. Unwanted radiation from the earth and atmosphere are suppressed by the use of stray light features that are critical to mission success. These include the use of an intermediate field stop, an inner and outer Lyot stop, and super-polished mirrors. The point source normalized irradiance transmission (PSNIT) curve, which characterizes the sensor's off-axis response, was computed using the stray light analysis program APART. An initial calculation of the non-rejected radiance (NRR) due to emissions and scatter from the earth and atmosphere was made using the PSNIT data. The results indicate that stray light will not impede the mission objectives.

Keywords: stray light analysis, baffle design, Lyot stop, triple diffraction, APART, ASAP, BRDF, PSNIT, SABER, TIMED

1. INTRODUCTION

The Sounding of the Atmosphere using Broadband Emission Radiometry (SABER) instrument is part of the NASA Thermosphere-Ionosphere-Mesosphere Energetics and Dynamics (TIMED) mission, which is scheduled for launch in the year 2000. The sensor is a 10-channel earth limb-viewing sensor that is to measure atmospheric emissions in the spectral range of 1.27 μm to 16.9 μm. A 625 km orbit is planned. The channel specific species, spectral bandpass, and noise equivalent radiance (NER) are listed in Table 1. The telescope, shown in Figure 1, is an on-axis Cassegrain design with a picket-fence tuning fork chopper at the first focus, and a clamshell re-imager to focus the image on the focal plane. A single axis scan mirror is used to obtain vertical profiles of the earth's atmosphere. The instrument description and mission objectives are described in greater detail elsewhere[1-3]. A preliminary stray light analysis by Stauder[4] reported that SABER was well suited for its mission. At the time of the analysis, however, the telescope design and stray light model were not complete, resulting in an underestimation of the stray light. Important omissions from the earlier report were the modeling of the secondary support structure and obscuration stop. Diffraction from these components, along with that of successive system stops, proved to be substantial. To assure mission success, an innovative inner Lyot stop was added to the system to control most of the diffraction. This paper details the stray light design and analysis of SABER with an emphasis on design features not discussed in the preliminary report.

Table 1. SABER measured species, bandpass, and noise equivalent radiance (NER).

Channel Number	Species	Spectral Band (μm)	NER (W cm^{-2} sr^{-1})
1	CO_2 (N)	14.71 – 15.75	1.75E-8
2	CO_2 (W)	13.16 – 17.24	2.8E-8
3	CO_2 (W)	13.16 – 17.24	2.8E-8
4	O_3	8.77 – 9.90	1.12E-8
5	H_2O	6.41 – 7.25	3.73E-9
6	NO	5.19 – 5.63	2.49E-9
7	CO_2 (B)	4.17 – 4.41	1.32E-9
8	OH (A)	1.92 – 2.22	4.70E-10
9	OH (B)	1.55 – 1.74	7.00E-10
10	O_2	1.25 – 1.29	7.00E-10

Additional author information : Email: stauder@sdl.usu.edu; Telephone: 435-797-4388

Part of the SPIE Conference on Infrared Spaceborne Remote Sensing VI
San Diego, California • July 1998 SPIE Vol. 3437 • 0277-786X/98/$10.00

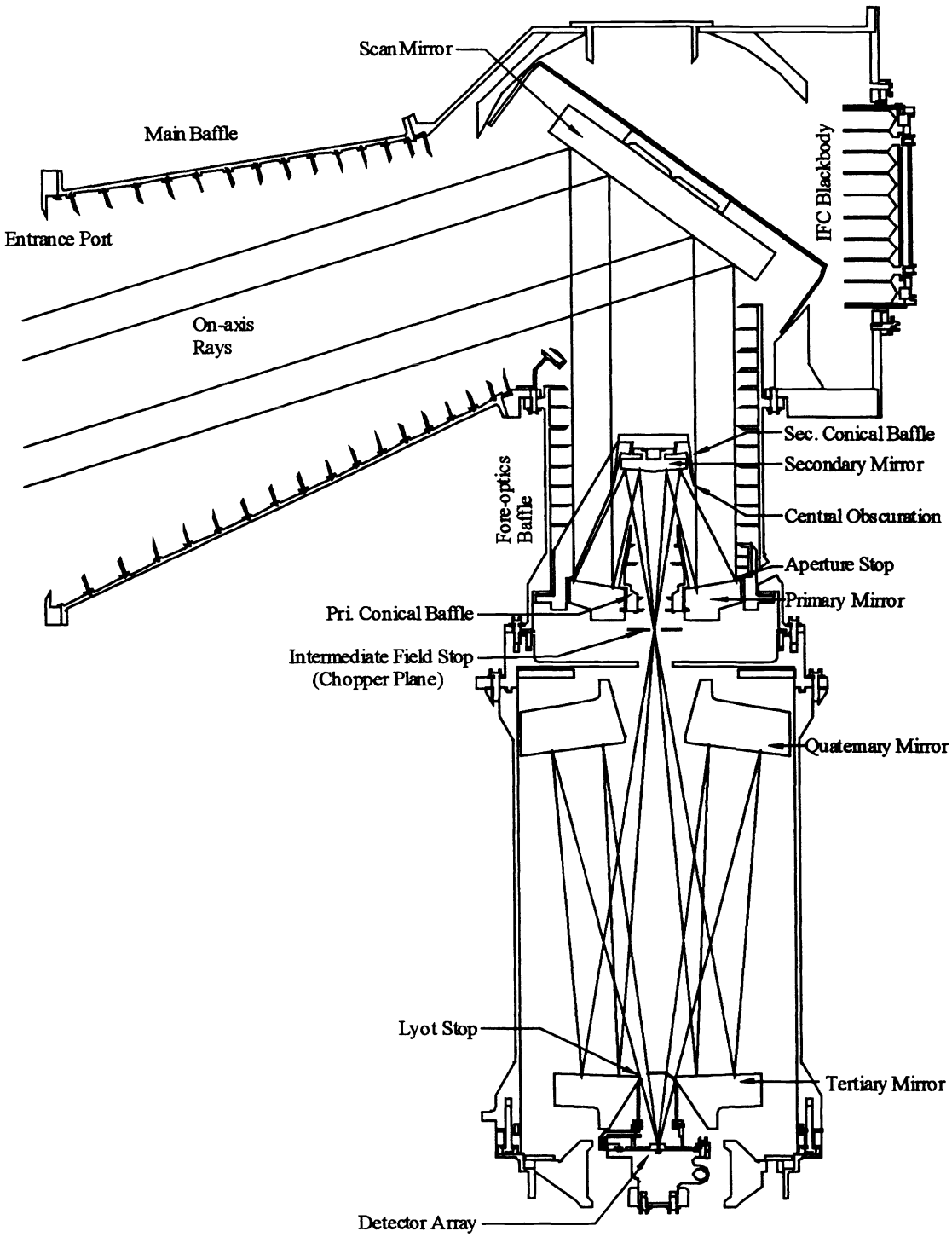

Figure 1. The SABER telescope.

2. STRAY LIGHT DESIGN

Stray light suppression in a sensor is best achieved through the iterative process of design and analysis. It is advantageous to begin this process early in the design of the telescope. Often a sensor is not analyzed for stray light until the design is complete and in production. Fixing a stray light problem is usually costly in both time and schedule, and rarely is the fix optimal. The iterative approach proved to be very beneficial, and necessary, to the SABER telescope as demonstrated by the inclusion of the inner Lyot stop.

The optimum stray light design for a given system requires minimizing the number of non-optical components that can be seen by the detector. The remaining elements that are in view of the detector, along with the optics, are called critical objects. The next step is to reduce, or eliminate, the off-axis power on these critical objects. The two important tasks listed above are best accomplished by the use of stops and baffles. A final step in the design process is to select the surface characteristics of mirrors and other components. Mirror scatter is often the greatest contributor of stray light in a well-designed system such as SABER. For this reason, all of SABER's mirrors were chosen to be super-polished and kept in a class 100 clean room environment through launch. Non-optical components are coated with a highly absorbing black paint. Light that is not absorbed is ideally scattered uniformly in all directions.

2.1 Use of and placement of system stops

The use of and placement of stops in a system is often the most important stray light design decision to be made. The aperture stop, whose main function is to limit the incoming ray bundle, has a much greater purpose in terms of stray light suppression. When used correctly, it will reduce the number of critical objects, thus minimizing unwanted power on the detector. It is best to place the stop as deep in the optical path as possible. The field stop defines the field-of-view (FOV) of the sensor. When possible, the field stop is most effective if placed forward in the optical path. Re-imaging systems allow for the use of an intermediate field stop and a Lyot stop. The field stop is best located at the first image plane of the system. Only scattered or diffracted light from elements located prior to the field stop can penetrate deeper into the system. The Lyot stop is placed at the image of the aperture stop, and is slightly undersized to become the *effective* aperture stop of the system. Since diffracted light originating from the aperture stop is imaged onto the Lyot stop, nearly all of it will be blocked prior to reaching the detector. Located deep in the optical path, the stop minimizes the number of critical objects. For unobscured systems, non-optical components preceding the Lyot stop in optical space will not be imaged onto the detector.

On-axis reflective systems such as SABER pose challenges not encountered in off-axis designs. Stray light paths result from the centrally located secondary mirror, secondary conical baffle (SCB), and support structure. The conventional, or outer, Lyot stop discussed above provides no protection here. Diffraction from the secondary support edges and the SCB tip, which functions as the inner aperture stop, were major stray light sources for the longer wavelength channels of SABER. At all wavelengths, scattered light from the inside surface of the SCB imaged by the primary and secondary mirrors onto the detector was significant. The detector could also view the inner and outer surfaces of the primary conical baffle (PCB) in reflection off the secondary mirror. The additional power on the focal plane due to the diffraction and scatter paths outlined above could not be tolerated. The solution to the problem is to make both the SCB and PCB surfaces non-critical objects by blocking their scattering path to the detector. This is realized by placing a disk deep into the system where the image of the inner aperture stop forms. The disk is called an inner Lyot stop since its placement is analogous to that of the outer Lyot stop. In addition to blocking SCB and PCB scatter, the inner Lyot stop removes diffraction from the inner aperture stop since it is slightly oversized.

Reduction of scatter and diffraction from the secondary support struts is achieved as follows. The sides of the three struts are rendered non-viewable to the detector by making the struts wedge-shaped, with the wide side of the wedge facing the primary mirror. Diffraction from the strut edges is removed by placing the supports of the inner Lyot stop at the images of the wide end of each strut. The supports are slightly over-sized. The flight Lyot stop assembly of SABER is shown in Figure 2.

Figure 2. SABER Lyot stop.

2.2 Baffle design

Reducing the off-axis power on the optical elements is the primary objective of a baffle. SABER's main baffle is extended to the maximum allowable length to minimize the range of angles an off-axis source can illuminate the scan, primary, and secondary mirrors. The baffle vanes are laid out to meet the two-bounce criteria, which requires incident light to be reflected off a vane or wall at least two times prior to striking the scan mirror. Each time a light ray encounters a painted vane, is loses energy due to absorption. After two or more reflections, or bounces, the radiation reaching the mirror is typically weakened several orders of magnitude. The same criterion was applied to the fore-optics baffle, where the primary mirror is the baffle's object of protection.

3. STRAY LIGHT ANALYSIS

The SABER telescope was analyzed for stray light using Arizona's Program for the Analysis of Radiation Transfer (APART[5]) and the Advanced Systems Analysis Program (ASAP[6]). The APART analysis was performed by Space Dynamics Laboratory (SDL). Breault Research Organization (BRO) conducted the ASAP analysis under contract to SDL. The analysis was separated into the near-field and far-field off-axis regions having a transition at 1 degree from the detector center FOV. ASAP is better suited for the near-field diffraction calculations. Scatter and far-field diffraction analysis is more efficiently handled by APART.

3.1 ASAP analysis

The sole purpose of the ASAP analysis was to calculate the near-field diffraction for various image points on the chopper plane. The diffraction calculations were made at 15.2 μm, which is the center wavelength of channel 1. The analyzed stray light path is known as triple diffraction and has serious implications not only in the near-field, but for all source angles where the primary stop is illuminated. The diffraction path involves the system stops and is outlined below in section 3.3. The reader is referred to Caldwell[7] for a more comprehensive treatment of the problem. The ASAP analysis of SABER has been reported on by Peterson[8] and is the subject of a future SPIE paper.

3.2 APART analysis

The far-field analysis performed in APART includes both scatter and diffraction effects. Required input to the model is the scattering properties of the mirrors and non-optical surfaces. The mirrors are characterized by the bi-directional reflectance distribution function (BRDF). Surface reflectivity is the parameter used for the non-optical surfaces including the baffle vanes. Scatter from the baffle vane edge tips is proportionate to its surface area, which is defined by tip radius. The tips have been measured and a radius of 0.05 mm was used in the analysis.

3.2.1 Mirror BRDF model

The BRDF estimates of the mirrors used in the previous stray light report of SABER were better than the BRDF of the flight mirrors. This added to the underestimation of unwanted power on the focal plane. BRDF measurements were made at the wavelengths of 1.55 μm, 3.39 μm, and 10.6 μm for the scan, primary, and secondary mirrors. Data was collected at five locations on each mirror, leading to an average BRDF value. Linear regression was used to fit a line to the averaged data. The results for the scan mirror at 10.6 μm are given in Figure 3. The BRDF at 1° was determined to be 1.26E-3 with a slope of –2.16. The BRDF of all the mirrors increased as the measured wavelength decreased. The BRDF values at 1° ranged from 3.37E-4 with a slope of –2.31 (primary mirror at 10.6 μm), to 2.61E-2 with a slope of –2.54 (scan mirror at 1.55 μm). The 10.6 μm derived data was used in the APART model for SABER channels 1 through 4. Channels 5, 6, and 7 received the 3.39 μm BRDF derived values, whereas channels 8, 9, and 10 were assigned the 1.55 μm data. BRDF measurements were not made for the tertiary and quaternary mirrors. Estimates based on the manufacturer's specifications were assigned to these mirrors for the APART analysis.

3.2.2 Painted surface model

The baffle vanes and other non-optical components of SABER that receive light are painted with Aeroglaze Z-306. The surface is modeled as being perfectly diffuse having a reflectivity ranging from 6 to 10 percent, depending on the channel wavelength. The paint does exhibit a specular component especially for the longer wavelength channels, thus indicating the importance for the baffles to meet the two-bounce criteria. It is impractical to model the specular component of Z-306 for the baffle vanes in APART.

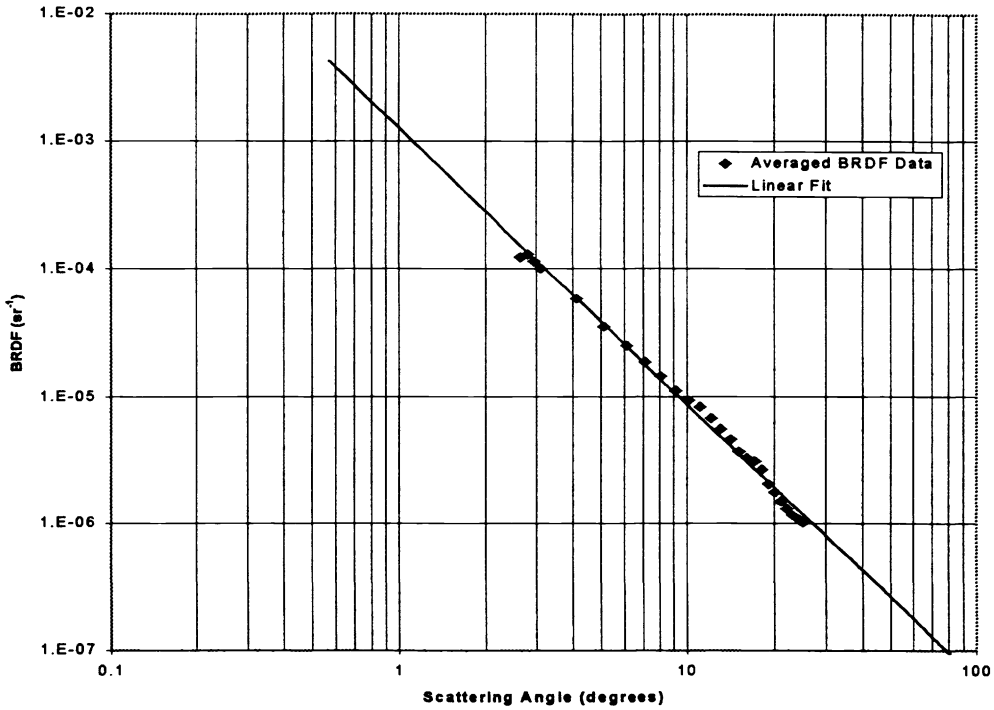

Figure 3. BRDF data of scan mirror measured at 10.6 μm.

3.3 Tripple diffraction

The combined diffraction from successive stops in a re-imaging system is termed "triple diffraction". The propagation of energy through a generalized system is depicted in Figure 4. The first diffraction occurs at the aperture stop, where the ray bundle from a distant off-axis point source is clipped. The resulting point spread function (PSF) is centered about the geometrical image of the source, located at point A in the figure. The side lobes of the PSF are spread across the field stop opening where the second diffraction takes place. This produces a "PSF ring" with a peak centered about the geometrical image of the aperture stop indicated by point B on the Lyot stop. Since the point source is off-axis, the energy in the central lobe is not uniform around the ring. It is however, symmetric. The undersized Lyot stop blocks the central lobe, which is characteristic of a well-baffled system. The third diffraction, resulting from the energy spread across the Lyot stop, is distributed onto the focal plane as shown. It appears as a bright ring surrounding the detector having a peak centered at point C, which is the geometrical image of the circular field stop. The energy in the side lobes incident on the detector is the amount of stray light contributed by the triple diffraction effect.

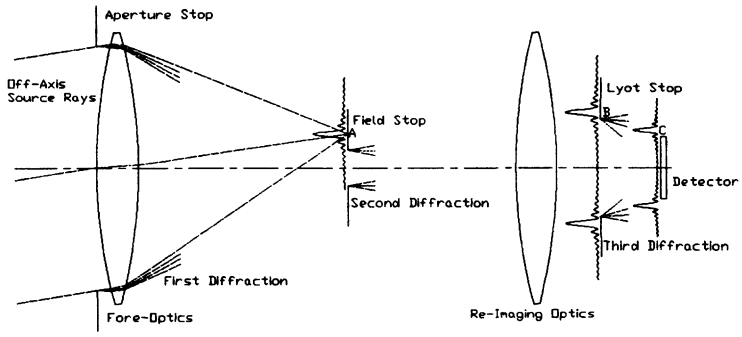

Figure 4. Triple diffraction propagation in a generalized system.

The triple diffraction analysis for SABER is more complicated than indicated above due to the presence of the picket-fence chopper located at the first image plane. The 10 rectangular openings are each matched to a detector element at the final image plane. In essence, each opening is the field stop for the corresponding detector. At the maximum open position, the holes are slightly oversized in relation to the detectors. Thus, the diffraction spread across each detector due to the corresponding chopper hole is similar to that shown in Figure 4. The only difference is that the PSF peak appears as a bright rectangle instead of a ring. As the chopper hole closes, the main peak contracts around and eventually slides across the detector. Initially this produces an increase in stray light. However, since the energy contained in the PSF fringes across the chopper hole is decreasing, at some point the power on the detector subsides. The presence of a diffraction peak on the detector, which originates from an off-axis source, is not desirable. The diffraction is worse for the longer wavelength channels and when the stray light source is less than 1° from the detector FOV. Fortunately for SABER, the near-field stray light can be calibrated out from the desired signal. Another disadvantage of having multiple field stops is that diffraction from one hole can spread across all of the detectors. For a given detector, this non-signal hole contribution is significantly smaller than the diffraction from the signal chopper hole. However, non-signal hole diffraction cannot effectively be calibrated out.

4. INSTRUMENT CHARACTERIZATION AND PERFORMANCE

The point source normalized irradiance transmittance (PSNIT) function is used to characterize the off-axis response of SABER. The PSNIT is defined as the irradiance on the detector due to an off-axis source divided by the source irradiance at the entrance port, which is 1 Watt/mm^2 in the APART analysis. The response of channel 10 looking at a tangent height of 70 km will be used to illustrate the stray light mechanisms present in SABER for the shorter wavelength channels. The PSNIT is depicted in Figure 5, and is representative of channels 8, 9, and 10. The sampled data begins at 1° from the detector optical axis, which is offset from the main baffle centerline by 4.6°. Below, the off-axis angles are given with respect to the baffle axis. Occasionally an angle is given in parenthesis to denote the angle with respect to the detector axis. At off-axis angles of 20° and less, scattered light from the scan, primary, and secondary mirrors that is imaged onto the detector is the dominant source of stray light. As the point source moves off-axis, the mirrors are gradually shielded from the source. The angles at which the scan, primary, and secondary mirrors are no longer illuminated are 25°, 15°, and 10°, respectively. At 5.6° (1°), the

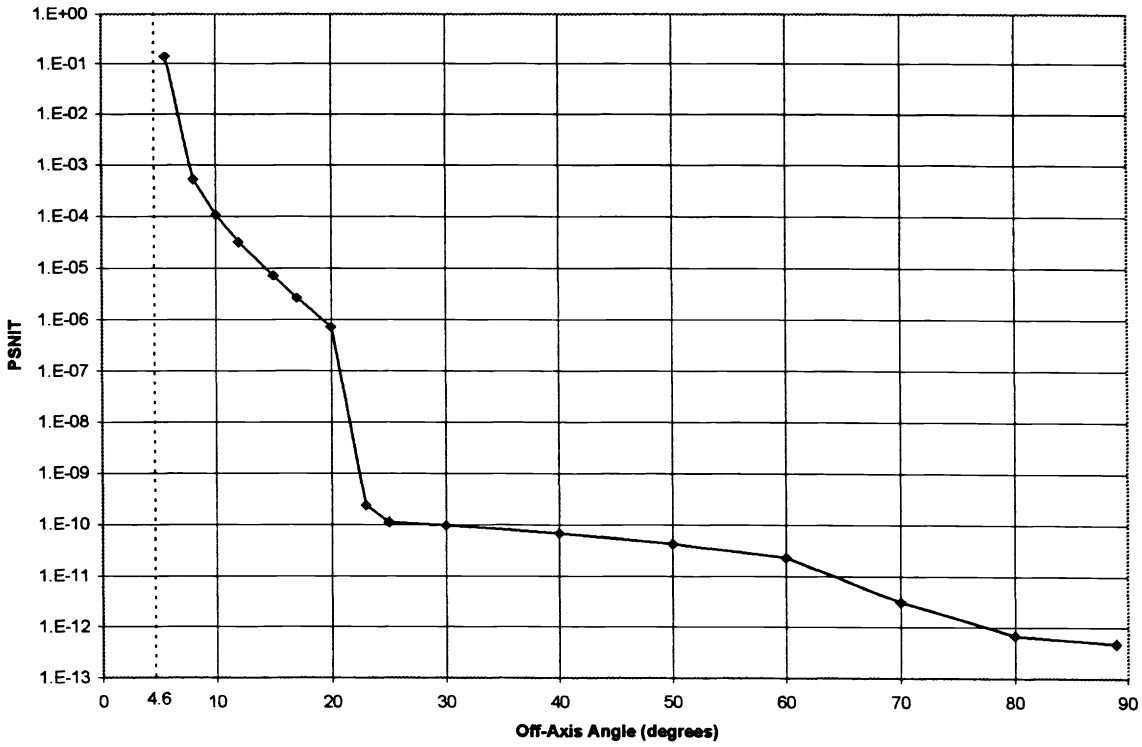

Figure 5. PSNIT for channel 10 looking at 70 km.

scatter contribution is evenly distributed between the three mirrors. Beyond 5.6°, the scan mirror becomes the main contributor since it is shielded at a slower pace than the two other mirrors. The response slowly decreases with increasing off-axis angle until the scan mirror is totally shielded from the point source by the main baffle. The rapid drop in the response between 20° and 25° indicates where complete shielding takes place. Following this drop, multiple scattering paths involving the scan mirror account for the majority of the response. The paths include diffraction from the entrance port edge and scatter off the main baffle vanes, which in turn scatter off the scan mirror onto the detector. To a lesser extent, multiple paths resulting in scatter from the primary and secondary mirrors is present. The steady decline in the response between 25° and 60° results from a decreasing illumination of the main baffle vanes. The steeper drop in the response from 60 to 80 degrees indicates that scatter from the front portion of the baffle is less important than scatter from the vanes nearer to the scan mirror.

The analysis above shows that scatter from the mirrors dominates the stray light for the short wavelength channels, thus indicating the importance of super-polished mirrors. Diffraction played a relatively minor role. This is not the case for the long wavelength channels where diffraction is more pronounced. The off-axis response of a longer wavelength channel is discussed for a comparison to the shorter wavelength channels. The PSNIT of channel 1 looking at 70 km is given in Figure 6. It is representative of SABER channels 1 through 4. The APART generated data begins at 6.5° with respect to the main baffle axis, which corresponds to 1° from the detector center FOV. The on-axis data point at 5.5° is from the ASAP analysis. At off-axis angles up to and including 15°, portions of the primary stop are illuminated. Unlike the channel 10 response, triple diffraction is the major contributor in this region. Mirror scatter becomes significant at 10° (4.5°), and slows the rapid drop due to diffraction. After 15° (9.5°), the drop in response picks up since the primary stop and mirror are no longer directly illuminated by the source. The rapid drop continues between 20° and 25° as the scan mirror becomes shielded from the source. Stray light paths involving multiple diffraction and scatter accounts for the remaining response. The wavelength dependence on the PSNIT curves described above is substantial. The shorter wavelength channels are dominated by mirror scatter due to a larger BRDF and smaller diffraction component. Conversely, the longer wavelength channels are heavily depended on the triple diffraction path. Not surprisingly, the off-axis response for the mid-wavelength channels (5, 6, and 7) is more evenly dependent on mirror scatter and diffraction.

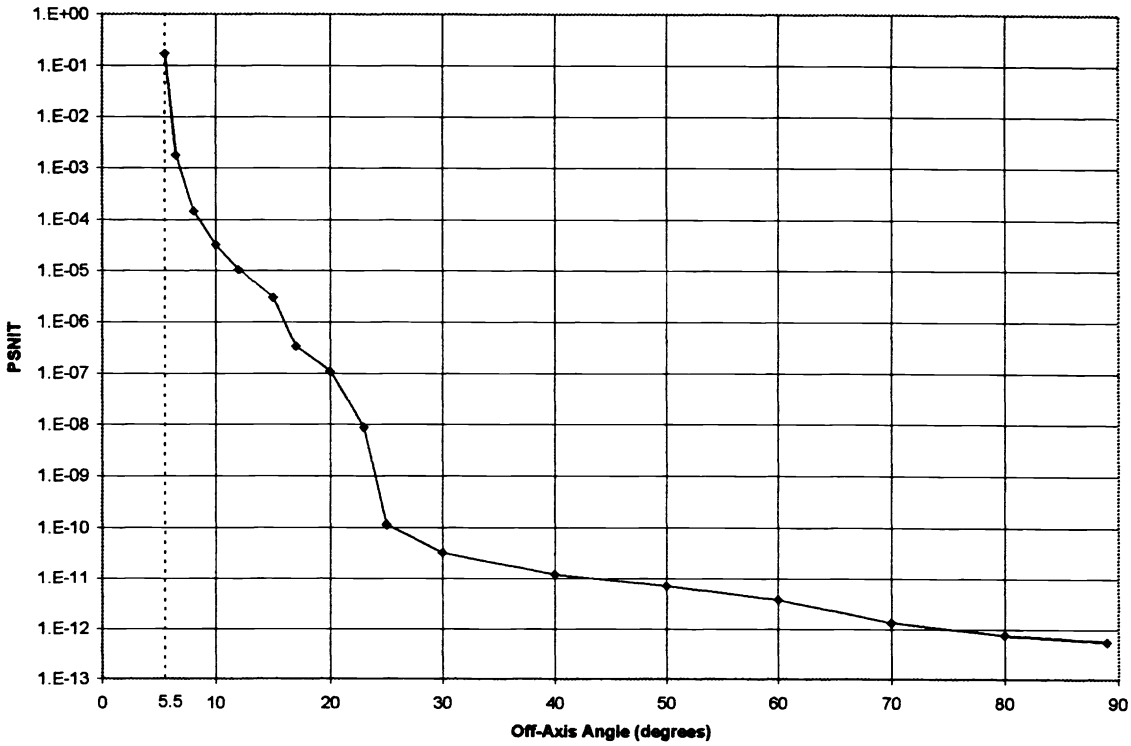

Figure 6. PSNIT for channel 1 looking at 70 km.

5. FUTURE ANALYSIS

The stray light analysis of SABER is still ongoing as of this writing. The final calculation of stray light on the detector array due to emissions from the earth and atmosphere is near completion. This contribution is measured in terms of the non-rejected radiance (NRR), which is calculated by using the PSNIT curve and radiance data provided by Gordley *et. al*[9]. The integration is described in detail by Stauder *et. al*[4]. The NRR will be calculated for each channel as a function of tangent height and compared to the channel specific NER and expected signal radiance. Earlier results for channel 1 looking at 70 km will be used here as an example. Using both the APART and ASAP PSNIT data, the NRR-to-NER ratio was determined to be 1.84. The signal radiance-to-NRR ratio, i.e. signal to noise ratio (SNR), is 119. When signal processing is used to correct for the near-field diffraction, the NRR/NER and SNR are 0.232 and 941, respectively. This particular result is somewhat optimistic since the goal BRDF values were used in earlier calculation of the PSNIT. Future plans call for the off-axis measurement of the SABER telescope in the Space Dynamics Laboratory off-axis chamber described by Kemp[10]. The measurement will be made using a visible source and should verify the APART computer analysis of the short wavelength channels.

6. CONCLUSIONS

The analysis presented in this paper gives an indication that SABER will successfully register the desired atmospheric emissions in the presence of unwanted radiation from the earth and atmosphere. For the channels where the stray light is expected to exceed the NER, the signal strength should be adequate to make the required measurement. The estimation of stray light will not be complete, however, until the final NRR calculations are made. Only then can exact conclusions be made. Data processing techniques will be utilized to correct for the near-field diffraction on the longer wavelength channels. The iterative process of design and analysis was used to improve the stray light suppression of the SABER telescope. Most important of the new features are the addition of the inner Lyot stop and the placement of its supports. The main source of stray light for the longer wavelength channels was found to be diffraction. Mirror scatter is the dominant source at the shorter wavelengths. To ensure mission success, stringent contamination control is required through launch. Any degradation of the mirror BRDF will have an effect on measurements made by the short and middle wavelength channels.

7. REFERENCES

1. R. Esplin *et. al.*, "SABER instrument overview", *Infrared Spaceborne Remote Sensing II*, Proc. SPIE Vol. 2268, pp. 207-217, 1994.
2. R. Esplin *et. al.*, "SABER instrument design update", *Infrared Spaceborne Remote Sensing III*, Proc. SPIE Vol. 2553, pp. 253-263, 1995.
3. "SABER Critical Design Review (CDR)", 1997.
4. J. Stauder *et. al.*, "Stray light analysis of the SABER telescope", *Infrared Spaceborne Remote Sensing III*, Proc. SPIE Vol. 2553, pp. 264-270, 1995.
5. "APART stray light analysis software package, Version 9.7a", Breault Research Organization 6400 East Grant Road, Suite 350, Tucson Arizona, 85715.
6. "ASAP optical systems analysis software package, Version 5.1", Breault Research Organization 6400 East Grant Road, Suite 350, Tucson Arizona, 85715.
7. M. Caldwell, P.Gray, "Application of a generalized diffraction analysis to the design of nonstandard Lyot-stop systems for earth limb viewing radiometers", *Optical Engineering*, **36**(10) pp. 2793-2808, 1997.
8. G. Peterson, "ASAP analysis of triple diffraction stray light in the SABER system", Breault Research Organization report no. 3310, February 3, 1998.
9. L. Gordley, B. Marshall, and D. Chu, "LINEPAK: Algorithm for modeling spectral transmittance and radiance", *J. Quant. Spectrosc. Radiat. Transfer*, 52, pp. 563-580, 1994.
10. J. Kemp, *et. al.*, "Terrestrial "Back Hole" for measuring high-rejection off-axis response", *Infrared Spaceborne Remote Sensing V*, Proc. SPIE Vol. 3122, pp. 45-56, 1997.